

## SIMULATED OBSERVATIONS OF SMALL BODIES: THE EFFECT OF SHAPE AND TOPOGRAPHY

S.M. Potin<sup>1</sup>, S. Douté<sup>2</sup>, B. Kugler<sup>3</sup>, F. Forbes<sup>3</sup>, <sup>1</sup>Centre for Terrestrial and Planetary Exploration (C-TAPE), University of Winnipeg, 515 Portage Avenue, Winnipeg, Manitoba R3B 2E9, Canada; <sup>2</sup>Université Grenoble Alpes, CNRS, Institut de Planétologie et d'Astrophysique de Grenoble (IPAG).; <sup>3</sup>Université Grenoble Alpes, CNRS, Inria, Grenoble INP, Laboratoire Jean Kuntzmann (LJK), Grenoble, France ; (sandra.potin63@gmail.com).

**Introduction:** Reflectance spectroscopy is a common tool used to retrieve physical and mineralogical information on Solar System planetary bodies. However, the reflectance spectrum of a surface depends on several parameters, including the illumination condition and observing geometry [1]. The observed reflectance of small bodies is generally compared to laboratory measurements of meteoritic samples or terrestrial analogues to assess the composition and alteration history of the target's surface. Laboratory measurements are performed in a controlled environment, where the composition and texture of the sample are known and the illumination and observing geometry is fixed. However, if the spectroscopic observations of the small body are unresolved, its reflectance is integrated over the whole observed surface, which averages spatial compositional and textural heterogeneities and changes in the illumination and observation geometries due to both the shape of the object and the topography of its surface (slopes, craters, ...).

Here we use spectral bidirectional reflectance of terrestrial analogues measured in the laboratory and applied on 3D models of the planetary bodies (1) Ceres and (4) Vesta. We simulate the observation of these bodies by a spacecraft during a fly-by, and compare them with the spectroscopic results obtained in the laboratory.

### Samples, measurements and inversion model:

We consider two different samples, a fine powder of a howardite and a highly porous foam-like sublimation residue of a Ceres simulant [2]. The laboratory Bidirectional Reflectance Distribution Function (BRDF) measurement, and inversion procedure used to model the reflectance of the surface under any triplet of incidence, emergence, and phase angles are described in [3].

**Simulation of the observations:** We apply the BRDF model of the howardite and the sublimation residue on each facet of a shape model of (4) Vesta and (1) Ceres, respectively. The whole surfaces of the simulated bodies are thus homogeneously covered with the material studied in the laboratory. We then simulate the fly-by of a spacecraft near these simulated objects. The created planetary body and the direction of illumination is fixed, so that the subsolar point is at the same position of the surface of the object on each

observation. The spacecraft flies following a linear trajectory and observes the surface, pointing at the center of the body at each time. Pictures are acquired under phase angles spanning 6° to 135°. We use a simple pinhole camera model providing 90x90 pixels images with a spatial scale of 0.067°/pixel [4]. For each simulated object, we obtain 10 spectral image cubes acquired under various phase angles (Fig. 1).

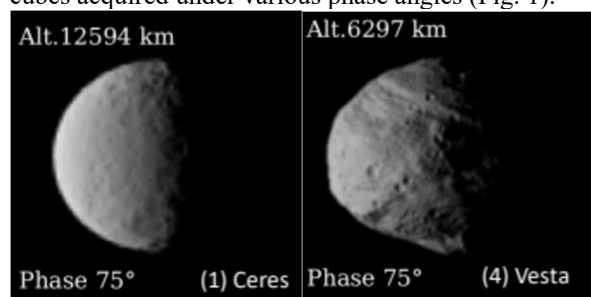


Fig. 1: Examples of radiance images of the simulated (1) Ceres covered with the sublimation residue and (4) Vesta covered with the fine powder of howardite. Observations at 400nm under a phase angle of 75°.

**Unresolved spectroscopy:** In case of unresolved observations, the reflectance spectroscopy of the target is integrated over the whole body, thus averaging all geometrical configurations induced by the shape and surface topography. We then compare the unresolved photometric and spectroscopic phase curves of the simulated (1) Ceres and (4) Vesta with the results obtained in the laboratory on the howardite and sublimation residue.

**Photometry:** We first compare the variations of the reflectance in the visible with increasing phase angle.

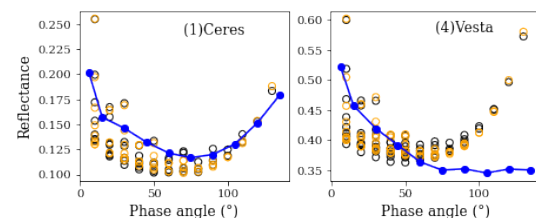


Fig. 2: Photometric phase curves at 0.7 $\mu$ m of the simulated (1)Ceres (left panel) and (4)Vesta (right panel). Blue: Integrated reflectance of the simulated target, Black: reflectance measured in the laboratory, Orange: reflectance derived from the spectral inversion by the RTLSR model.

The phase curve of the simulated Ceres matches the laboratory results of its surface in reflectance value and evolution with increasing phase angle. The simulated Ceres presents however a reflectance value slightly higher than what has been measured in the laboratory, while staying in the range of the measurements.

In contrast, the phase curve of the simulated Vesta presents a different behavior with increasing phase angle compared to the laboratory measurements. The reflectance measured on the powder of howardite increases along with phase angle from 60°, while the integrated reflectance only decreases monotonically with the phase angle. This specific behavior traces the dominance in this phase angle range of the shadowing effects due to multiple roughness scales in the topography of the surface. A similar behavior that was modelled by [5] is observed for the Moon and is due to the quasi-fractal structure of the regolith [6].

*Spectral slope and band depth:* We consider the spectral slope as the ratio between the reflectance observed at two well-separated wavelengths, divided by the difference between the wavelengths. The variations of the spectral slope with increasing phase angles are presented in Fig. 3.

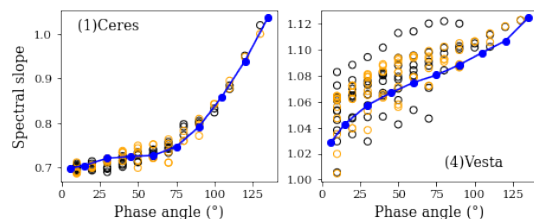


Fig. 3: Phase curves of the spectral slope of the simulated (1) Ceres (left panel) and (4) Vesta (right panel). The slopes are calculated on the integrated reflectance spectra of the simulated targets (blue), on the reflectance spectra measured in the laboratory (black) and derived from the spectral inversion (orange).

We calculate the band depth as the ratio between the measured reflectance and the value of a linear continuum at the wavelength corresponding to the minimum of reflectance inside the absorption band. The variations of the 3- $\mu\text{m}$  band depth with increasing phase angle are presented in Fig. 4.

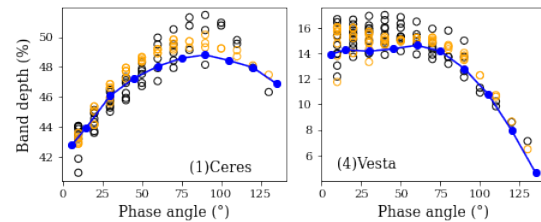


Fig. 4: Phase curves of the 3- $\mu\text{m}$  band depth of the simulated (1) Ceres (left panel) and (4) Vesta (right panel). The band depths calculated on the integrated reflectance spectra of the simulated targets (blue), on the reflectance spectra measured in the laboratory (black) and derived from the spectral inversion (orange).

The spectral slope and band depth phase curves of both simulated objects match the laboratory results and spectral inversion. However, the spectral parameters measured on the integrated spectra tend to be slightly lower than what can be measured in the laboratory or resulting from the inversion. While the photometric phase curve of an unresolved body can be affected by the topography of the surface and differs from the phase curves of the surface applied on it, the other spectral parameters seem to be a better point of comparison.

**Conclusion:** We applied the composition and texture of samples measured in the laboratory on shape models of planetary bodies. We then simulated the unresolved observations of these bodies by a spacecraft flying by, and compared the results to the laboratory measurements. We showed that the integrated reflectance of a body can be impacted by the topography of the surface and thus differ from the laboratory measurements of the same surface while the derived spectral slope and band depth are less affected.

**References:** [1] Potin et al. (2019) *Icarus*, 333, 415-428.. [2] Schröder et al. (2021) *Nature Com.*, *in press*. [3] Potin et al. (2020), EPSC Abstracts, EPSC2020-201 [4] Zienleniewski et al. (2015) *M.N.R.A.S.*, 453, 3754-3765. [5] Shkuratov, and Helfenstein (2001), *Icarus*, 152, 96-116. [6] Helfenstein, P., and J. Veverka (1987) *Icarus* 72, 342-357.